Title

Tris(1,3-dichloro-2-propyl) phosphate disrupts cellular metabolism within human embryonic kidney (HEK293) cells.

Authors

Avila-Barnard, Sarah

Ha, Megan

Nemarugommula, Charvita

et al.

Publication Date

2024-03-15

DOI

10.1016/j.jhazmat.2024.133660

Peer reviewed

HHS Public Access

Author manuscript

J Hazard Mater. Author manuscript; available in PMC 2024 March 15.

Published in final edited form as:

J Hazard Mater. 2024 March 15; 466: 133660. doi:10.1016/j.jhazmat.2024.133660.

Tris(1,3-dichloro-2-propyl) phosphate disrupts cellular metabolism within human embryonic kidney (HEK293) cells

Sarah Avila-Barnard[a], **Megan Ha**[a], **Charvita Nemarugommula**[a], **Jenna L. Wiegand**[a], **Haiyan Ke**[b], **Amancio De Souza**[b], **Rachel Behar**[c], **David C. Volz**[a,*]

[a] Department of Environmental Sciences, University of California, Riverside, CA 92521, USA

[b] Metabolomics Core Facility, Institute for Integrative Genome Biology, University of California, Riverside, CA, USA

[c] Stem Cell Core Facility, University of California, Riverside, CA, USA

Abstract

Tris(1,3-dichloro-2-propyl) phosphate (TDCIPP) is a widely used, additive flame retardant that migrates from end-use products, leading to ubiquitous exposure of humans around the world. However, little is known about whether TDCIPP disrupts the physiology of human embryonic cells. Therefore, the objective of this study was to determine whether TDCIPP alters cell viability, cellular metabolism, cytosine methylation, and reactive oxygen species (ROS) levels within human embryonic kidney (HEK293) cells. Relative to vehicle controls, TDCIPP (0.015–0.1225 μM) resulted in a concentration-dependent increase in cell viability, a finding that was driven by an increase in relative ATP abundance. Interestingly, TDCIPP (0.061–0.98 μM) increased the rate of glycolysis – an adaptive mechanism consistent with the Warburg effect exhibited by tumorigenic cells. Moreover, relative to vehicle-treated cells, TDCIPP (0.245–15.63 μM) exposure for 48 h (but not 24 h) resulted in a significant, concentration-dependent decrease in ROS in situ, and TDCIPP (0.245 μM) exposure significantly increased carnosine within the histidine metabolism pathway. However, TDCIPP did not affect global 5-methylcytosine (5-mC) methylation (0.015–15.63 μM), cell membrane integrity (0.061–0.98 μM), nor the abundance of mitochondria (0.061–1.95 μM). Overall, our findings with TDCIPP point to a novel mechanism of action that may be relevant to human embryonic stem cells.

GRAPHICAL ABSTRACT

* Corresponding author. david.volz@ucr.edu (D.C. Volz).

Declaration of Competing Interest

The authors declare that they have no known competing financial interests or personal relationships that could have appeared to influence the work reported in this paper.

CRediT authorship contribution statement

Volz David: Conceptualization, Funding acquisition, Project administration, Resources, Supervision, Writing – review & editing. **Wiegand Jenna:** Investigation, Methodology. **Nemarugommula Charvita:** Investigation, Methodology. **Ha Megan:** Investigation, Methodology. **Avila-Barnard Sarah:** Conceptualization, Formal analysis, Investigation, Methodology, Validation, Visualization, Writing – original draft, Writing – review & editing. **Behar Rachel:** Investigation, Methodology. **De Souza Amancio:** Investigation, Methodology. **Ke Haiyan:** Investigation, Methodology.

Appendix A. Supporting information

Supplementary data associated with this article can be found in the online version at doi:10.1016/j.jhazmat.2024.133660.

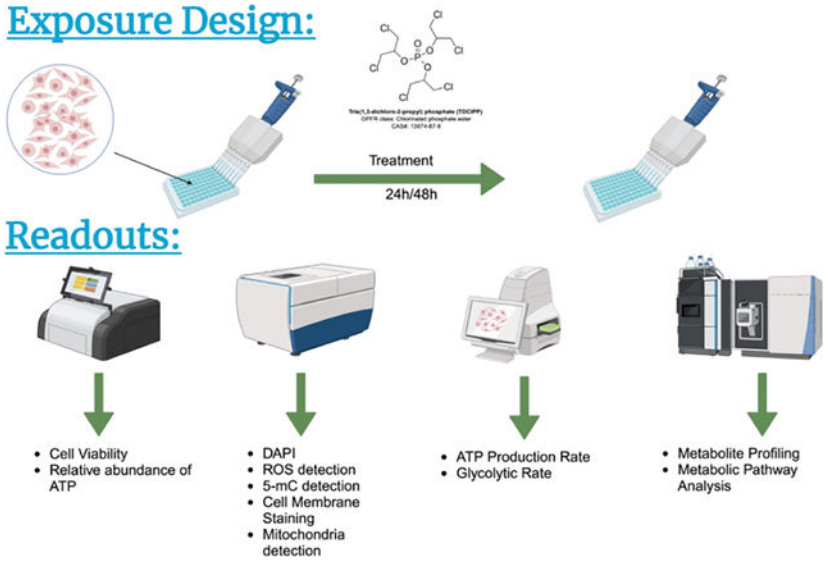

Keywords

TDCIPP; HEK293 cells; Metabolism; ATP; Warburg effect; Reactive oxygen species

1. Introduction

Tris(1,3-dichloro-2-propyl) phosphate (TDCIPP) is an additive organophosphate-based flame retardant widely used around the world within products such as polyurethane foam. As these products age, TDCIPP has the potential to migrate from end-use products into environmental media such as air, dust, and surface water. Within the United States, TDCIPP has been detected in serum, urine, hair, breast milk, and placental tissues [1–4]. Although TDCIPP rapidly metabolizes into mono- or diester metabolites that are excreted in urine, the high frequency of TDCIPP detection in urine is due to ubiquitous exposure in our surrounding environment [5,6] via multiple routes of exposure including inhalation, ingestion, and dermal absorption [3]. Although the use of TDCIPP in upholstered furniture has declined within California, TDCIPP is still prevalent within the indoor environment due to its presence within a variety of existing consumer products including vehicles.

In 2011, TDCIPP was added to California's Proposition 65 (Prop 65) list based on its potential to cause cancer following ingestion [7]. In addition to being a suspected carcinogen, TDCIPP impacts DNA methylation within zebrafish and mice during early embryonic development [8–12]. Moreover, TDCIPP has been associated with adverse pregnancy outcomes within human cohorts [13–15]. To our knowledge, no studies in the peer-reviewed literature have investigated the potential effects of TDCIPP within human embryonic cells and only a limited number of studies have characterized the potential toxicity of TDCIPP within cell lines derived from pediatric patients (SH-SY5Y neuroblastoma cells) [16] and adult patients (SMMC-7721 hepatocellular carcinoma cells, NCI-1975 non-small cell lung cancer cells, normal corneal epithelial cells, and HK-2 papillomavirus 16-transformed kidney proximal tubule cells) [17–20]. Interestingly, across

all five studies, TDCIPP induced reactive oxygen species (ROS) production, apoptosis, and cytotoxicity within five different human cell lines, albeit the lowest concentration that induced toxicity was highly variable (1–300 μM) and dependent on the duration of exposure (24- vs. 72-h exposure). For 24-h exposures, the lowest concentrations that induced toxicity were 1, 25, 100, and 300 μM for SMMC-7721 cells [17], SH-SY5Y cells [16], HK-2 papillomavirus 16-transformed kidney proximal tubule cells [19], and normal corneal epithelial cells [18], respectively. For a 72-h exposure, the lowest concentration that induced toxicity was 50 μM for NCI-1975 cells [20].

Overall, prior studies suggest that TDCIPP-induced oxidative stress may be a common mechanism of action within human cells, although the sensitivity of different cell lines to TDCIPP is highly variable and no studies to date have investigated the effects of TDCIPP within human embryonic cells. Therefore, the overall objective of this study was to address how TDCIPP exposure affects the physiology of human embryonic kidney (HEK293) cells by assessing cell viability, ATP production, reactive oxygen species (ROS) generation, as well as the abundance of 5-methylcytosine (5-mC), cell membranes, and mitochondria in situ. Although HEK293 cells are tumorigenic and do not recapitulate the normal biology of cells derived from human embryos, we utilized HEK293 cells as a model to begin investigating the potential impacts of TDCIPP on cellular metabolism within cells originally derived from human embryos, as human embryonic stem cells are cost-prohibitive and require days to weeks to differentiate.

2. Materials and methods

2.1. Chemicals

TDCIPP (99% purity) was purchased from Chem Service, Inc. (West Chester, PA). A mother stock solution of 50 mM TDCIPP was prepared in high-performance liquid chromatography (HPLC)-grade dimethyl sulfoxide (DMSO) and stored within 2-mL amber glass vials with polytetrafluoroethylene-lined caps. Additional stock solutions ranging from 0.015–31.25 mM TDCIPP were prepared by diluting the 50 mM mother stock solution into 100% DMSO within 2-mL amber glass vials with polytetrafluoroethylene-lined caps. Working solutions were prepared by spiking 1 μL of stock solutions into 999 μL of sterile cell culture media immediately prior to each exposure, resulting in 0.1% DMSO within all vehicle and treatment groups.

2.2. HEK293 cell culture

HEK293 cells were purchased from American Type Culture Collection (ATCC) (Manassas, VA, USA) and grown in Eagle's Minimum Essential Medium (ATCC, Manassas, VA, USA) supplemented with 10% fetal bovine serum (FBS) (ATCC, Manassas, VA, USA). Cells were maintained in a temperature- and CO_2-controlled incubator at 37 °C and 5%, respectively. Cell culture media was changed every 48 h and cells were split at 70–90% confluency every four to five days (depending on confluency) using 0.25% Trypsin/0.53 EDTA (ATCC, Manassas, VA, USA).

2.3. Cell viability assay

HEK293 cells were counted using a hemocytometer and resuspended in 20 mL of sterile cell culture media at a concentration of ~1×10^6 and ~5×10^5 cells for 24-h and 48-h exposures, respectively. 200 μL of HEK293 cells were plated in sterile 96-well plates at a final concentration of ~1×10^4 and ~5×10^3 cells per well for 24-h and 48-h exposures, respectively, and allowed to adhere overnight. Media was then removed from each well and replaced with 200 μL of media containing either vehicle (0.1% DMSO) or TDCIPP (0.015, 0.031, 0.061, 0.1225, 0.245, 0.49, 0.98, 1.95, 3.91, 7.81, 15.63, and 31.25 μM) within four replicate wells per treatment. Cells were then incubated at 37 °C and 5% CO_2 for 24 h or 48 h. In addition, blank wells (media alone with cells) and negative control wells (media alone without cells) were also included to account for any DMSO-specific effects and/or background fluorescence, respectively. At the end of the exposure duration, the plate was allowed to equilibrate to room temperature. Treatment solutions were removed from all wells and replaced with 100 μL of sterile cell culture media (warmed to room temperature) and 100 μL of CellTiter-Glo (CTG) reagent (Promega, Madison, WI, USA). The plate was mixed on an orbital shaker for 2 min to induce cell lysis and then allowed to incubate at room temperature for 10 min to allow luminescence to stabilize. Luminescence was then measured using a GloMax-Multi + Detection Dual Injector System (Promega, Madison, WI, USA).

2.4. Pre-treatment with oligomycin or compound 3 K

To determine the maximum tolerated concentration (MTC), HEK293 cells were plated and pre-treated for 12 h as described above to either vehicle (0.1% DMSO), oligomycin (an ATP synthase inhibitor), or compound 3 K (a pyruvate kinase M2, or PKM2, inhibitor) using the following concentrations: 0.05, 0.10, 0.50, or 1 μM. 1 μM was used as an upper limit, as previous studies found that 1 μM was sufficient to successfully disrupt mitochondrial or glycolytic activity without inducing cytotoxicity [21–23]. The exposure solution was aspirated from each well, replaced with 4% paraformaldehyde (PFA) for 5 min at room temperature, and washed three times for 5 min with 1X phosphate-buffered saline (PBS). Cells were then counterstained with a 1:4 solution of DAPI Fluoromount-G (Southern Biotechnology, Birmingham, AL) for 5 min at room temperature on an orbital shaker (100 rpm). Cells were washed three times for 5 min with 1X PBS at room temperature before being preserved in 250 μL of 1X PBS. Cells were then imaged at 10X magnification under a DAPI filter using our ImageXpress Micro XLS Widefield High-Content Screening System. Within MetaXpress 6.0.3.1658, each well was analyzed for total fluorescence area intensity using custom automated image analysis procedures. After exporting data from MetaXpress into Excel files, R coding along with packages *deployer* and *writexl* were used to sort, and summate data points for each well, filter by well number, and export summated data output from MetaXpress into an Excel file.

Cells were pre-treated with vehicle (0.1% DMSO), the MTC of oligomycin, or the MTC of compound 3 K for 12 h, and then cells were exposed to vehicle (0.1% DMSO) or TDCIPP (0.061, 0.245, or 0.98 μM) for either 24 h or 48 h. Untreated and negative control wells were utilized to account for any vehicle-specific effects. Each treatment group was conducted in replicates of eight. At the end of the exposure, four replicate wells were utilized for each

treatment group. After aspirating the exposure solution from each well, cells were fixed with 4% PFA, counterstained with DAPI, preserved, and imaged as described above. For the remaining four replicates, a CTG assay was used to determine cell viability. CTG-based luminescence data were normalized to DAPI total area to account for any variability in the number of cell nuclei.

2.5. Seahorse XFp analyzer assays

2.5.1. Real-time ATP rate assay—We relied on a Seahorse XFp Real-Time ATP Rate Assay Kit (Agilent, Wilmington, DE) as a broad approach to quantify the rate of ATP production from glycolysis and mitochondrial respiration in live cells. HEK293 cells were plated in a Seahorse XFp cell culture miniplate (~4 $\times 10^3$ cells per well in 80 μL) and allowed to adhere overnight in a 37°C CO_2 incubator. HEK293 cells were exposed to vehicle (0.1% DMSO) or TDCIPP (0.015, 0.98, and 3.91 μM) for 24 h using methods described above (three replicate wells per treatment group). Per the manufacturer's instructions, the sensor cartridge was hydrated one day prior to the assay at 37°C in a non-CO_2 incubator overnight using sterile molecular grade biology (MGB) water. On the day of the assay, MGB water was discarded from the utility plate and replaced with prewarmed XF Calibrant 50 min prior to loading the ports. Under sterile conditions, assay media was created by supplementing 10 mL of Seahorse XF DMEM Medium (pH=7.4) with 10 mM of XF glucose, 1 mM of XF pyruvate, and 2 mM of XF glutamine and then warmed to 37°C in a non-CO_2 incubator. At exposure termination, cells were removed from a 37°C CO_2 incubator and examined under a microscope for confirmation of consistent plating and proper cell morphology. Cells were then washed with warmed Seahorse media and transferred to a non-CO_2 incubator for incubation at 37°C for 45 min prior to the assay. As cells were incubating, fresh stock compound solutions of oligomyocin (75 μM) and rotenone + antimycin A (24 μM) were prepared and vortexed for ~1 min before being diluted to 1.5 μM and 0.5 μM, respectively. Diluted stock solutions were then added to their respective ports in the sensor cartridge and placed in the Seahorse XFp analyzer for calibration. After 45 min, cells were washed with warmed assay media prior to being placed in the Seahorse XFp analyzer and initiating the assay. Oxygen consumption rate (OCR) and extracellular acidification rate (ECAR) were recorded for each well. Seahorse media was then aspirated from each well and replaced with 200 μL of Hoechst 33342 dye diluted in Seahorse media for a final concentration of 0.002 μM per well. The plate was then placed in a non-CO_2 37 °C incubator for 5 min. Cells were then imaged on a Nikon Eclipse TI under a DAPI filter using a 10X objective and exported as a TIFF file for each replicate well. Each TIFF file was then imported into ImageJ to count the total number of detectable cells. OCR and ECAR rates were then imported into ImageJ to count the total number of detectable cells. OCR and ECAR rates were then normalized by their respective cell counts and initial readings for each time point.

2.5.2. Glycolytic rate assay—We relied on a Seahorse XFp Glycolytic Rate Assay Kit (Agilent, Wilmington, DE) as a targeted approach to quantify a potential shift from basal to compensatory glycolysis. HEK293 cells were plated in a Seahorse XFp Microplate (~4 $\times 10^3$ cells per well) and then allowed to adhere overnight in a 37°C CO_2 incubator. Non-treated and blank wells were used to account for any vehicle-specific effects or background noise.

We exposed cells to either vehicle (0.1% DMSO) or TDCIPP (0.061, 0.245, and 0.98 μM) for 24 h using methods described above. As cells incubated, fresh stock compound solutions of rotenone + antimycin A (50 μM) and 2-deoxy-D-glucose (500 mM) were reconstituted and vortexed for ~1 min before being diluted to 0.5 μM and 50 mM, respectively, in warmed seahorse media. We then quantified OCR, ECAR, and proton efflux rate (PER) through real-time measurements of changes in glycolytic rates in vehicle-vs. TDCIPP-treated cells using a Seahorse XFp Analyzer. Cells were then stained with Hoechst as well as imaged and analyzed as described above.

2.6. CellROX green assay

Detailed methods are provided within the Supplemental Material.

2.7. Central carbon metabolism-specific metabolomics

Cells were plated and exposed as described above. For analysis of biomolecules involved in central carbon metabolism, cells were exposed to either vehicle (0.1% DMSO) or TDCIPP (0.061, 0.245, or 0.98 μM) for 24 h (96 wells pooled per replicate; four replicates per treatment). At exposure termination, treatment solutions were aspirated and replaced with 50 μL of a 1:2 dilution of Trysin-EDTA in cell culture media. Cells were then incubated for 3–5 min at 37 °C before adding 100 μL of media to deactivate trypsin. Trypsinized cells (96 wells per replicate) were washed and then transferred into a 15-mL tube. Cells were centrifuged for 10 min at 1.2 rpm, and the supernatant was discarded and replaced with 200 μL of Hank's Balance Salt Solution (HBSS). The cell pellet was washed by gentle agitation and centrifuged for 10 min at 1.2 rpm, and cells were washed and centrifuged two more times.

On the third wash, 10 μL was removed from each sample to perform a cell count using a hemocytometer and a 1:1 dilution of Trypan Blue (Thermo Fisher Scientific, Waltham, MA). Cells were then centrifuged for 20 min at 1.2 rpm. HBSS was removed and replaced with 50 μL of chilled 100% methanol. Cells were stored at − 80 °C overnight. On the following day, samples were sonicated for 10 min in an ice bath, vortexed, and sonicated for 5 min or until the cell pellet was completely disrupted. Samples were then centrifuged for 20 min at 4000 rpm and 4 °C in 15 mL falcon tubes. The supernatant was then aspirated, transferred to an amber glass vial, and a nitrogen blower was used to evaporate the methanol. Samples were resuspended in 50 μL of methanol and then processed by UCR's Metabolomics Core Facility using a Waters TQ-XS triple quadrupole mass spectrometer coupled to a Waters two-dimensional I-class UPLC.

Targeted metabolomics of polar, primary metabolites were performed at UCR's Metabolomics Core Facility as previously described [24]. Briefly, the analysis was performed on a TQ-XS triple quadrupole mass spectrometer (Waters, Milford MA) coupled to an I-class UPLC system (Waters, Milford MA). Separations were carried out on a ZIC-pHILIC column (2.1 ×150 mm, 5 μM) (EMD Millipore, Burlington, MA). The mobile phases were A) water with 15 mM ammonium bicarbonate adjusted to pH 9.6 with ammonium hydroxide and B) acetonitrile. The flow rate was 200 μL/min and the column was held at 50 °C. The injection volume was 2 μL. The gradient was as follows: 0 min,

90% B; 1.5 min, 90% B; 16 min, 20% B; 18 min, 20% B; 20 min, 90% B; 28 min, 90% B. The MS was operated in multiple reaction monitoring mode (MRM). Source and desolvation temperatures were 150 °C and 600 °C, respectively. Desolvation gas was set to 1100 L/hr and cone gas to 150 L/hr. Collision gas was set to 0.15 mL/min. All gases were nitrogen except the collision gas, which was argon. Capillary voltage was 1 kV in positive ion mode and 2 kV in negative ion mode. A quality control (QC) sample, generated by pooling equal aliquots of each sample, was analyzed periodically to monitor system stability and performance. Samples were analyzed in random order.

2.8. 5-methylcytosine (5-mC) Immunocytochemistry, cell membrane labeling, and mitotracker orange staining

Detailed methods are provided within the Supplemental Material.

2.9. Statistical analyses

A general linear model (GLM) analysis of variance (ANOVA) (α=0.05) and Tukey-based multiple comparisons were performed using SPSS Statistics 24 for detecting significant differences between treatment groups for cell viability, CellROX-Green, Seahorse, MitoTracker Orange, WGA, and 5-mC IHC data. For the metabolomics data, we assessed all detectable metabolites that were statistically different in TDCIPP-treated groups relative to the vehicle control using a confidence interval between 80–95% confidence (α=0.05, 0.1, and 0.2).

3. Results

3.1. TDCIPP increases cell viability at concentrations < 1 μM

Relative to vehicle-treated cells, exposure to TDCIPP for 24 h or 48 h resulted in a significant concentration-dependent increase in cell viability up to 0.98 μM (Fig. 1). However, higher concentrations of TDCIPP (>1 μM) did not increase nor decrease cell viability relative to vehicle-treated cells (Fig. 1). Interestingly, relative to 48 h of exposure, the magnitude of the effect of TDCIPP on cell viability was higher following 24 h of exposure. Pre-treatment with an ATP synthase inhibitor (oligomycin) and PKM2 inhibitor (compound 3 K) alone up to 1 μM did not affect the total number of HEK293 cells (Fig. S1), albeit there was a slight non-significant decrease in cell viability at 1 μM. Therefore, we relied on 0.1 μM as the MTC for oligomycin and compound 3 K to minimize the possibility of cytotoxicity or off-target effects prior to TDCIPP exposures. However, pre-treatment with 0.1 μM oligomycin or 0.1 μM compound 3 K did not mitigate TDCIPP-induced effects on cell viability across all three concentrations at 24 h nor 48 h (Fig. 2), suggesting that TDCIPP-induced enhancement of cell viability was not mediated by direct or indirect activation of ATP synthase or PKM2.

3.2. TDCIPP increases the rate of glycolysis

Based on the broad ATP production rate assay, exposure for 24 h to TDCIPP (0.061, 0.245, and 0.98 μM) did not significantly affect ECAR (glycolysis) nor OCR (mitochondrial respiration) within live HEK293 cells relative to vehicle-treated cells (Fig. 3), albeit there was a non-significant increase in ECAR (glycolysis) following exposure to 0.245

μM TDCIPP after injection of rotenone/antimycin A. Interestingly, based on a targeted glycolytic rate assay that can more precisely detect a shift from basal to compensatory glycolysis, exposure for 24 h to TDCIPP resulted in a significant increase in ECAR and PER relative to vehicle-treated cells after injection of rotenone/antimycin A (Fig. 4), suggesting that TDCIPP exposure for 24 h increased the rate of glycolysis within live HEK293 cells. Although there was not a clear concentration-response relationship between the concentration of TDCIPP and glycolytic rate of HEK 293 cells, effects on glycolysis were, like the ATP rate assay, more pronounced following exposure to 0.245 μM TDCIPP.

3.3. TDCIPP decreases intracellular ROS and impacts the histidine metabolism pathway

Although 24 h of exposure resulted in no effect on ROS, there was a statistically significant, concentration-dependent decrease in ROS (relative to vehicle-treated cells) after 48 h of exposure starting at 0.245 μM TDCIPP (Fig. 5). ROS approached levels within blanks (untreated cells) by 3.91 μM TDCIPP (Fig. 5), suggesting that 1) exposure to 0.1% DMSO alone may increase ROS generation within HEK293 cells and 2) TDCIPP may counteract the effects of 0.1% DMSO. Overall, these data indicate that 48 h of continuous TDCIPP exposure may decrease ROS from 0.245–15.63 μM relative to vehicle-treated cells.

Interestingly, relative to vehicle-treated cells, exposure for 24 h to 0.245 μM TDCIPP resulted in alterations in biomolecules involved in central carbon metabolism that were statistically significant at an $\alpha = 0.05$, 0.1, or 0.2 (Fig. 6), with carnosine being the most significantly affected. In addition, we found significant impacts of TDCIPP on the histidine metabolism pathway, with a specific increase in intracellular carnosine levels following exposure to 0.245 μM TDCIPP (Fig. 7). These data suggest that TDCIPP exposure up to 24 h resulted in an increase in intracellular carnosine and impacts the histidine metabolism pathway within HEK293 cells, although this effect is strongly dependent on the TDCIPP concentration.

3.4. TDCIPP does not affect 5-mC, cell membrane integrity, nor mitochondria in situ

TDCIPP exposure up to 15.63 μM for either 24 h or 48 h did not affect the abundance of 5-mC relative to vehicle-treated cells (Fig. S2). Exposure for either 24 h or 48 h TDCIPP (0.061, 0.245, and 0.98 μM) did not result in statistically significant differences relative to vehicle-treated cells (Fig. S3). In addition, pre-treatment with oligomycin or compound 3 K did not affect cell membrane integrity in the presence or absence of TDCIPP (Fig. S3). Exposure for either 24 h or 48 h to TDCIPP (0.061, 0.245, and 0.98 μM) did not result in statistically significant differences in the abundance of mitochondria relative to vehicle-treated cells (Fig. S4).

4. Discussion

Prior studies published in the peer-reviewed literature found that TDCIPP induces oxidative stress and cytotoxicity in human cells originally derived from pediatric and adult patients at concentrations ranging from 1–300 μM depending on the exposure duration (24- or 72-h exposure) [16–20]. However, contrary to all five prior studies, within this study we unexpectedly revealed that, within human embryonic cells (HEK293), TDCIPP increased

cell viability – rather than induced cytotoxicity – after 24 h and 48 h of exposure at concentrations (<1 μM) that are lower than any TDCIPP concentrations tested to date within human cell lines. Therefore, this raised the question of whether TDCIPP activated key ATP-producing enzymes, as the CTG assay is based on ATP quantification as a readout for metabolically active cells. However, pre-treatment with either oligomycin (an ATP synthase inhibitor) or compound 3 K (PKM2 inhibitor) did not mitigate TDCIPP-induced enhancement of cell viability, suggesting that TDCIPP did not increase the relative abundance of ATP via direct or indirect activation of key, rate-limiting enzymes – ATP synthase and PKM2 – involved in intracellular ATP production. Therefore, we relied on a Seahorse XFp Analyzer to determine whether TDCIPP increased the rate of ATP production via mitochondrial respiration or glycolysis within live HEK293 cells.

While TDCIPP had no effect on ATP production via mitochondrial respiration, we found that TDCIPP increased the rate of glycolysis (albeit in the absence of a clear concentration-response relationship), suggesting that a TDCIPP-induced increase in cell viability at TDCIPP concentrations < 1 μM may have been driven by an increase in ATP production via glycolysis. Interestingly, these findings are consistent with the Warburg effect that is exhibited by tumorigenic cells such as HEK293 cells [25–27]. Originally postulated in 1923, the Warburg effect is an adaptive mechanism that accelerates the conversion of glucose to lactate in malignant tumors via glycolysis [25], allowing tumorigenic cells to rapidly generate ATP in the presence or absence of functioning mitochondria and, as such, provide the bioenergetic demand needed to support uncontrolled proliferation and survival of tumor cells [25,26,28, 29]. Similarly, since mitochondrial function and the number of mitochondria in situ were not affected by TDCIPP, our data suggests that, even in the presence of functioning mitochondria, HEK293 cells increased the rate of glycolysis as an adaptive mechanism to support cell proliferation and survival in response to TDCIPP exposure.

Although TDCIPP did not affect global 5-mC methylation nor cell membrane integrity in situ, we found that TDCIPP decreased intracellular ROS within the same concentration range that increased cell viability and the rate of glycolysis. Within mitochondria, ROS species are created as by-products of cellular metabolism and play a role in oxidative reduction in the electron transport chain [30–32]. As ROS is utilized downstream for cellular signaling and redox signaling pathways, perturbations in the balance of mitochondrial ROS formation may negatively impact cell cycle checkpoints, cell proliferation, and cellular metabolism [33]. Indeed, as a result of increased glycolysis, the Warburg effect is known to disrupt mitochondrial redox potential, leading to a decrease in ROS generation by mitochondria [27,34]. Therefore, our findings suggest that a TDCIPP-induced increase in the rate of glycolysis may have decreased ROS generation within HEK293 cells by reducing the reliance on mitochondrial oxidative phosphorylation for ATP production.

Interestingly, we also found that TDCIPP significantly impacted the histidine metabolism pathway, with a specific increase in the levels of carnosine – a small molecule that is found in high levels in skeletal tissue and plays a role in antioxidant activity and scavenging carbonyls [35–37]. Within humans, histidine is an essential amino acid obtained from dietary sources and carnosine is synthesized from B-alanine and histidine by carnosine synthase within the cytosol [38]. Although carnosine decreases glycolytic ATP production

and proliferation of tumorigenic cells [39–41], we found that increased carnosine levels were associated with increased glycolysis and cell viability as well as decreased ROS, suggesting that the presence of higher levels of carnosine may have played a direct role in scavenging ROS rather than interfering with glycolysis. Overall, these findings support the conclusion that the metabolic environment of HEK293 cells was rewired in response to TDCIPP, another hallmark that is consistent with the Walburg effect within tumorigenic cells [27].

In summary, based on our results within human embryonic (HEK293) cells, our findings suggest that exposure to concentrations < 1 μM TDCIPP 1) increases cell viability; 2) increases the rate of glycolysis via the Warburg effect; 3) decreases mitochondrial ROS generation; and 4) increases carnosine levels within the histidine metabolism pathway. As a halogenated flame retardant, chlorine atoms on TDCIPP directly interact with and quench high energy free radicals produced in the vapor phase during combustion [42]. Therefore, following partitioning into HEK293 cells, there is a possibility that TDCIPP directly sequestered ROS which, in turn, decreased ROS levels, leading to disruption of the mitochondrial redox potential, ROS-mediated signaling pathways, and cellular metabolism (Fig. 8). Alternatively, as discussed above, TDCIPP may have directly induced the Warburg effect (i.e., an increased rate of compensatory glycolysis) and activated histidine metabolism pathways – both of which are adaptive mechanisms within tumorigenic cells that lead to decreased ROS generation (Fig. 8). Nevertheless, future studies are needed to further explore the underlying link between ROS generation and disruption of cellular metabolism by TDCIPP within human cells, including cancer cells and embryonic stem cells that may be more susceptible to the impacts of TDCIPP exposure.

Environmental Implication

Tris(1,3-dichloro-2-propyl) phosphate (TDCIPP) is an additive organophosphate flame retardant that is widely used within products such as textiles, plasticizers, and polyurethane foam. Within the United States, TDCIPP has been detected in breast milk and placental tissues. Although TDCIPP rapidly metabolizes into metabolites that are excreted in urine, the high frequency of TDCIPP detection in urine is due to its ubiquitous exposure in our surrounding environment. Overall, our findings with TDCIPP point to a novel mechanism of action that may be relevant to human embryonic stem cells and/or other organohalogen flame retardants that are frequently detected within human biomonitoring studies.

Supplementary Material

Refer to Web version on PubMed Central for supplementary material.

Funding

Fellowship support was provided by the NRSA T32 Training Program [T32ES018827] to SAB. Research support was provided by a National Institutes of Health grant (R01ES027576) and USDA National Institute of Food and Agriculture Hatch Project (1009609) to DCV.

Data availability

Data will be made available on request.

References

[1]. Yang J, Zhao Y, Li M, Du M, Li X, Li Y, 2019. A review of a class of emerging contaminants: the classification, distribution, intensity of consumption, synthesis routes, environmental effects and expectation of pollution abatement to organophosphate flame retardants (OPFRs). IJMS 20, 2874. 10.3390/ijms20122874. [PubMed: 31212857]

[2]. Ladd-Acosta C, 2015. Epigenetic signatures as biomarkers of exposure. Curr Envir Health Rpt 2, 117–125. 10.1007/s40572-015-0051-2.

[3]. Doherty BT, Hammel SC, Daniels JL, Stapleton HM, Hoffman K, 2019. Organophosphate esters: are these flame retardants and plasticizers affecting children's Health? Curr Environ Health Rep 6, 201–213. 10.1007/s40572-019-00258-0. [PubMed: 31755035]

[4]. Van Der Veen I, De Boer J, 2012. Phosphorus flame retardants: properties, production, environmental occurrence, toxicity and analysis. Chemosphere 88, 1119–1153. 10.1016/j.chemosphere.2012.03.067. [PubMed: 22537891]

[5]. Hoffman K, Butt CM, Webster TF, Preston EV, Hammel SC, Makey C, et al. , 2017. Temporal trends in exposure to organophosphate flame retardants in the United States. Environ Sci Technol Lett 4, 112–118. 10.1021/acs.estlett.6b00475. [PubMed: 28317001]

[6]. Chupeau Z, Bonvallot N, Mercier F, Le Bot B, Chevrier C, Glorennec P, 2020. Organophosphorus flame retardants: a global review of indoor contamination and human exposure in Europe and epidemiological evidence. IJERPH 17, 6713. 10.3390/ijerph17186713. [PubMed: 32942622]

[7]. Dodson RE, Perovich LJ, Covaci A, Van Den Eede N, Ionas AC, Dirtu AC, et al. , 2012. After the PBDE phase-out: a broad suite of flame retardants in repeat house dust samples from California. Environ Sci Technol 46, 13056–13066. 10.1021/es303879n. [PubMed: 23185960]

[8]. Yin S, Chen L, Wu D, Wang T, Huo L, Zhao S, et al. , 2019. Tris(1,3-dichloro-2-propyl) phosphate disturbs mouse embryonic development by inducing apoptosis and abnormal DNA methylation. Environ Mol Mutagen 60, 807–815. 10.1002/em.22322. [PubMed: 31411769]

[9]. Kupsco A, Dasgupta S, Nguyen C, Volz DC, 2017. Dynamic alterations in DNA methylation precede tris(1,3-dichloro-2-propyl)phosphate-induced delays in zebrafish epiboly. Environ Sci Technol Lett 4, 367–373. 10.1021/acs.estlett.7b00332. [PubMed: 28993812]

[10]. McGee SP, Cooper EM, Stapleton HM, Volz DC, 2012. Early zebrafish embryogenesis is susceptible to developmental TDCPP exposure. Environ Health Perspect 120, 1585–1591. 10.1289/ehp.1205316. [PubMed: 23017583]

[11]. Volz DC, Leet JK, Chen A, Stapleton HM, Katiyar N, Kaundal R, et al. , 2016. Tris(1,3-dichloro-2-propyl)phosphate induces genome-wide hypomethylation within early zebrafish embryos. Environ Sci Technol 50, 10255–10263. 10.1021/acs.est.6b03656. [PubMed: 27574916]

[12]. Avila-Barnard S, Dasgupta S, Cheng V, Reddam A, Wiegand JL, Volz DC, 2022. Tris(1,3-dichloro-2-propyl) phosphate disrupts the trajectory of cytosine methylation within developing zebrafish embryos. Environ Res 211, 113078. 10.1016/j.envres.2022.113078. [PubMed: 35248566]

[13]. Carignan CC, Mínguez-Alarcón L, Williams PL, Meeker JD, Stapleton HM, Butt CM, et al. , 2018. Paternal urinary concentrations of organophosphate flame retardant metabolites, fertility measures, and pregnancy outcomes among couples undergoing in vitro fertilization. Environ Int 111, 232–238. 10.1016/j.envint.2017.12.005. [PubMed: 29241080]

[14]. Carignan CC, Mínguez-Alarcón L, Butt CM, Williams PL, Meeker JD, Stapleton HM, et al. , 2017. Urinary concentrations of organophosphate flame retardant metabolites and pregnancy outcomes among women undergoing *in Vitro* fertilization. Environ Health Perspect 125, 087018. 10.1289/EHP1021 (for the EARTH Study Team). [PubMed: 28858831]

[15]. Hoffman K, Stapleton HM, Lorenzo A, Butt CM, Adair L, Herring AH, et al. , 2018. Prenatal exposure to organophosphates and associations with birthweight and gestational length. Environ Int 116, 248–254. 10.1016/j.envint.2018.04.016. [PubMed: 29698901]

[16]. Li R, Zhou P, Guo Y, Lee J-S, Zhou B, 2017. Tris (1,3-dichloro-2-propyl) phosphate-induced apoptotic signaling pathways in SH-SY5Y neuroblastoma cells. NeuroToxicol 58, 1–10. 10.1016/j.neuro.2016.10.018.

[17]. Guo M, Gu Y, Fan X, 2020. Chlorinated phosphorus flame retardants exert oxidative damage to SMMC-7721 human hepatocarcinoma cells. Sci Total Environ 705, 135777. 10.1016/j.scitotenv.2019.135777. [PubMed: 31972937]

[18]. Xiang P, Liu R-Y, Li C, Gao P, Cui X-Y, Ma LQ, 2017. Effects of organophosphorus flame retardant TDCPP on normal human corneal epithelial cells: implications for human health. Environ Pollut 230, 22–30. 10.1016/j.envpol.2017.06.036. [PubMed: 28641197]

[19]. Killilea DW, Chow D, Xiao SQ, Li C, Stoller ML, 2017. Flame retardant tris (1,3-dichloro-2-propyl)phosphate (TDCPP) toxicity is attenuated by N -acetylcysteine in human kidney cells. Toxicol Rep 4, 260–264. 10.1016/j.toxrep.2017.05.003. [PubMed: 28959647]

[20]. Meng Y, Xu X, Niu D, Xu Y, Qiu Y, Zhu Z, et al. , 2022. Organophosphate flame retardants induce oxidative stress and Chop/Caspase 3-related apoptosis via Sod1/p53/Map3k6/Fkbp5 in NCI-1975 cells. Sci Total Environ 819, 153160. 10.1016/j.scitotenv.2022.153160. [PubMed: 35051466]

[21]. Park JH, Kundu A, Lee SH, Jiang C, Lee SH, Kim YS, et al. , 2021. Specific pyruvate kinase M2 inhibitor, compound 3K, induces autophagic cell death through disruption of the glycolysis pathway in ovarian cancer cells. Int J Biol Sci 17, 1895–1908. 10.7150/ijbs.59855. [PubMed: 34131394]

[22]. Jastroch M, 2012. Expression of uncoupling proteins in a mammalian cell culture system (HEK293) and assessment of their protein function. In: Palmeira CM, Moreno AJ (Eds.), Mitochondrial Bioenergetics. Humana Press, Totowa, NJ, pp. 153–164. 10.1007/978-1-61779-382-0_10.

[23]. Chinthala Y, Sharma MKP, Kvn SS, Jonnala K, Arigari NK, Khan F, et al. , 2016. Synthesis and cytotoxicity evaluation of novel andrographolide-1,2,3-triazole derivatives. J Heterocycl Chem 53, 1902–1910. 10.1002/jhet.2505.

[24]. Vliet SMF, Dasgupta S, Sparks NRL, Kirkwood JS, Vollaro A, Hur M, et al. , 2019. Maternal-to-zygotic transition as a potential target for niclosamide during early embryogenesis. Toxicol Appl Pharmacol 380, 114699. 10.1016/j.taap.2019.114699. [PubMed: 31398420]

[25]. Vaupel P, Multhoff G, 2021. Revisiting the Warburg effect: historical dogma versus current understanding. J Physiol 599, 1745–1757. 10.1113/JP278810. [PubMed: 33347611]

[26]. Oronsky B, Oronsky N, Fanger G, Parker C, Caroen S, Lybeck M, et al. , 2014. Follow the ATP: tumor energy production: a perspective. ACAMC 14, 1187–1198. 10.2174/1871520614666140804224637.

[27]. Liberti MV, Locasale JW, 2016. The Warburg effect: how does it benefit cancer cells? Trends Biochem Sci 41, 211–218. 10.1016/j.tibs.2015.12.001. [PubMed: 26778478]

[28]. Zhu X, Xuan Z, Chen J, Li Z, Zheng S, Song P, 2020. How DNA methylation affects the Warburg effect. Int J Biol Sci 16, 2029–2041. 10.7150/ijbs.45420. [PubMed: 32549751]

[29]. Elia I, Haigis MC, 2021. Metabolites and the tumour microenvironment: from cellular mechanisms to systemic metabolism. Nat Metab 3, 21–32. 10.1038/s42255-020-00317-z. [PubMed: 33398194]

[30]. Forrester SJ, Kikuchi DS, Hernandes MS, Xu Q, Griendling KK, 2018. Reactive oxygen species in metabolic and inflammatory signaling. Circ Res 122, 877–902. 10.1161/CIRCRESAHA.117.311401. [PubMed: 29700084]

[31]. Thannickal VJ, Fanburg BL, 2000. Reactive oxygen species in cell signaling. Am J Physiol-Lung Cell Mol Physiol 279, L1005–L1028. 10.1152/ajplung.2000.279.6.L1005. [PubMed: 11076791]

[32]. Lyakhovich A, 2013. Damaged mitochondria and overproduction of ROS in Fanconi anemia cells. Rare Dis 1, e24048. 10.4161/rdis.24048. [PubMed: 25002988]

[33]. Brookes PS, Yoon Y, Robotham JL, Anders MW, Sheu S-S, 2004. Calcium, ATP, and ROS: a mitochondrial love-hate triangle. Am J Physiol-Cell Physiol 287, C817–C833. 10.1152/ajpcell.00139.2004. [PubMed: 15355853]

[34]. Ghanbari Movahed Z, Rastegari-Pouyani M, Mohammadi MH, Mansouri K, 2019. Cancer cells change their glucose metabolism to overcome increased ROS: one step from cancer cell to

cancer stem cell? Biomed Pharmacother 112, 108690. 10.1016/j.biopha.2019.108690. [PubMed: 30798124]

[35]. Babizhayev M, Lankin V, Savel'Yeva E, Deyev A, Yegorov Y, 2013. Diabetes mellitus: novel insights, analysis and interpretation of pathophysiology and complications management with imidazole-containing peptidomimetic antioxidants. DDF 7, 216–256. 10.2174/18722113076661311171210 58.

[36]. Barski OA, Xie Z, Baba SP, Sithu SD, Agarwal A, Cai J, et al. , 2013. Dietary carnosine prevents early atherosclerotic lesion formation in apolipoprotein E–null mice. ATVB 33, 1162–1170. 10.1161/ATVBAHA.112.300572.

[37]. Peters V, Klessens CQF, Baelde HJ, Singler B, Veraar KAM, Zutinic A, et al. , 2015. Intrinsic carnosine metabolism in the human kidney. Amino Acids 47, 2541–2550. 10.1007/s00726-015-2045-7. [PubMed: 26206726]

[38]. Brosnan ME, Brosnan JT, 2020. Histidine metabolism and function. J Nutr 150, 2570S–2575S. 10.1093/jn/nxaa079. [PubMed: 33000155]

[39]. Hipkiss AR, Gaunitz F, 2014. Inhibition of tumour cell growth by carnosine: some possible mechanisms. Amino Acids 46, 327–337. 10.1007/s00726-013-1627-5. [PubMed: 24292217]

[40]. Holliday R, McFarland G, 1996. Inhibition of the growth of transformed and neoplastic cells by the dipeptide carnosine. Br J Cancer 73, 966–971. 10.1038/bjc.1996.189. [PubMed: 8611433]

[41]. Renner C, Asperger A, Seyffarth A, Meixensberger J, Gebhardt R, Gaunitz F, 2010. Carnosine inhibits ATP production in cells from malignant glioma. Neurol Res 32, 101–105. 10.1179/016164109×12518779082237.

[42]. Shen J, Liang J, Lin X, Lin H, Yu J, Wang S, 2021. The flame-retardant mechanisms and preparation of polymer composites and their potential application in construction engineering. Polymers 14, 82. 10.3390/polym14010082. [PubMed: 35012105]

HIGHLIGHTS

- TDCIPP is a flame retardant with ubiquitous human exposure around the world.
- Little is known about TDCIPP-induced effects on human embryonic cells.
- TDCIPP increases the viability and rate of glycolysis within HEK293 cells.
- TDCIPP decreases mitochondrial ROS generation after 48 h of exposure.
- TDCIPP increases carnosine levels within the histidine metabolism pathway.

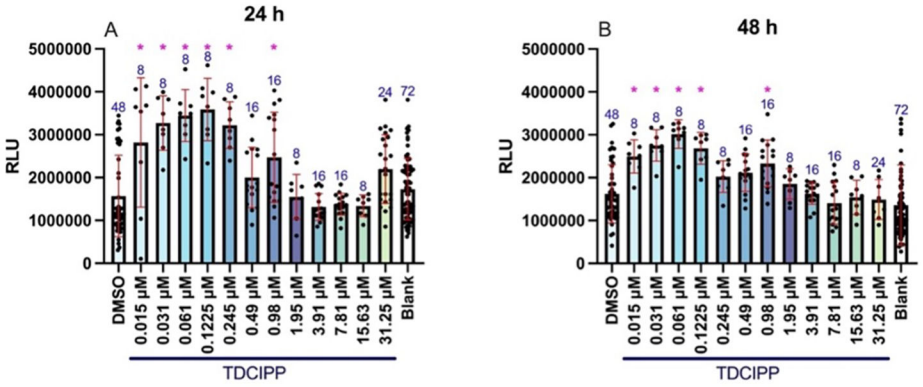

Fig. 1.

Mean (± standard deviation) CellTiter-Glo luminescence of HEK293 cells exposed to either vehicle (0.1% DMSO) or 0.015–31.25 µM TDCIPP for 24 h (A) or 48 h (B). Blank = unexposed cells. Sample sizes (number of wells) are indicated above each treatment group. Asterisk (*) denotes a significant difference ($p < 0.05$) relative to vehicle (0.1% DMSO).

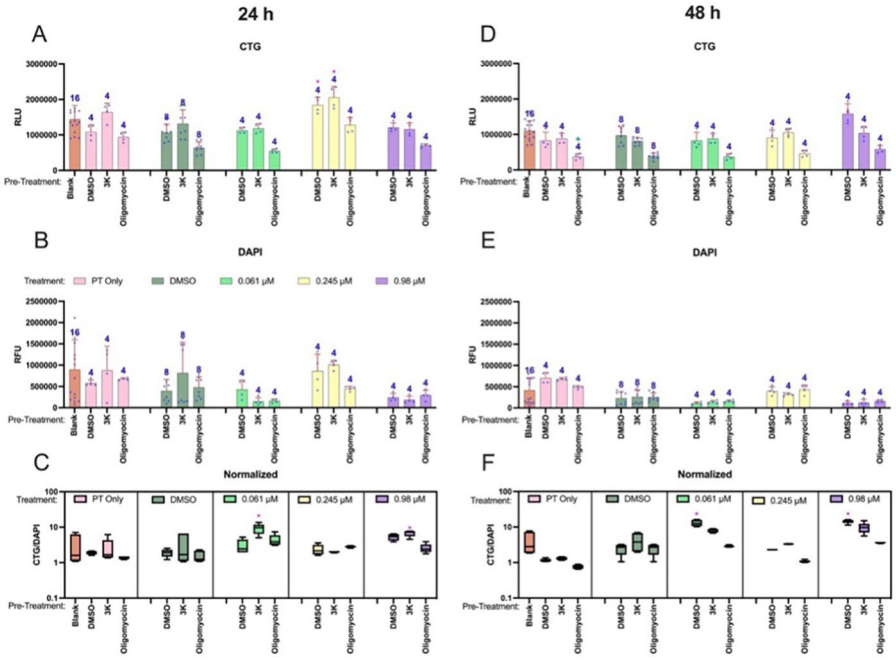

Fig. 2.

Mean (± standard deviation) CellTiter-Glo (CTG) luminescence (A, D), DAPI area (B, E), or DAPI-normalized CTG of HEK293 cells pre-treated with either vehicle (0.1% DMSO), oligomycin (0.1 µM), or compound 3 K (0.1 µM) for 12 h and then exposed to either vehicle (0.1% DMSO) or TDCIPP (0.061, 0.245, or 0.98 µM) for 24 h (A, B, C) or 48 h (D, E, F). Blank = unexposed cells. Sample sizes (number of wells) are indicated above each treatment group within Panels A, B, D, and E. Asterisk (*) denotes a significant difference ($p < 0.05$) relative to cells pre-treated with vehicle (0.1% DMSO) followed by exposure with vehicle (0.1% DMSO).

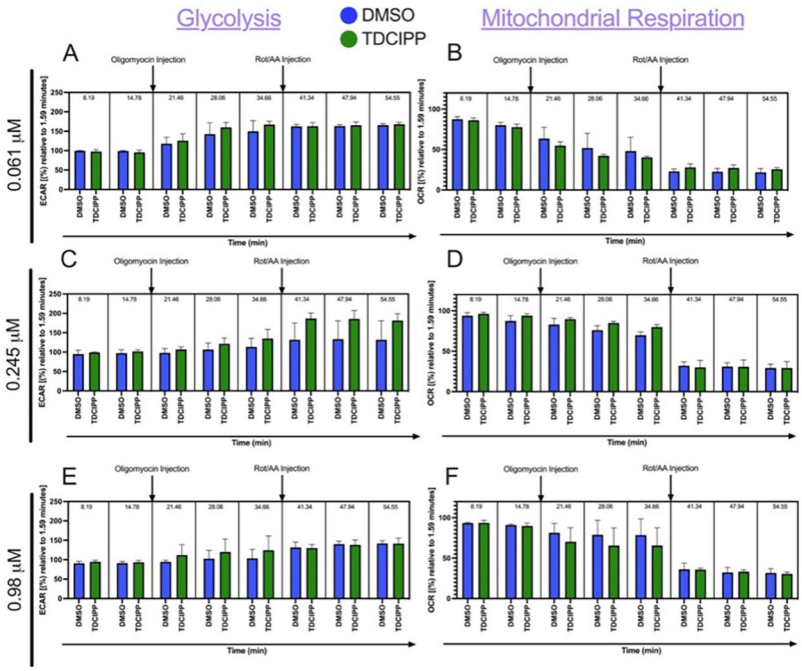

Fig. 3.

Mean extracellular acidification rate (ECAR) (A, C, E) and oxygen consumption rate (OCR) (B, D, F) of HEK293 cells exposed to either vehicle (0.1% DMSO) or TDCIPP (0.061, 0.245, or 0.98 µM) for 24 h. Asterisk (*) denotes a significant difference ($p < 0.05$) relative to vehicle controls.

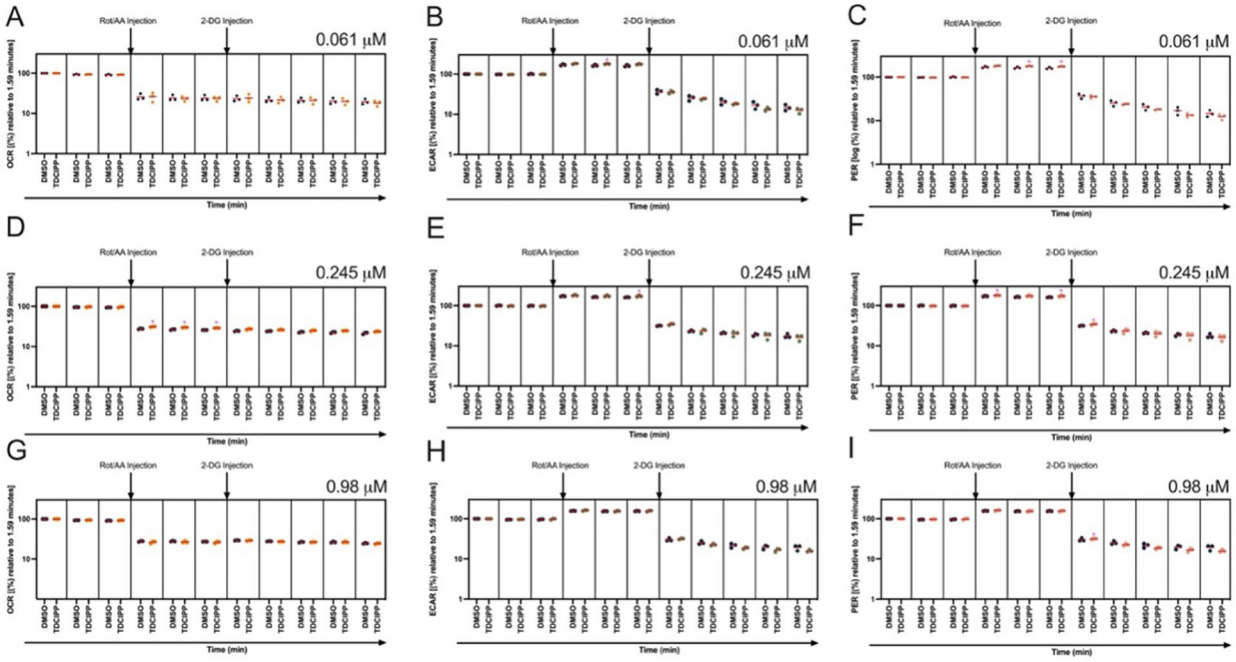

Fig. 4.

Mean oxygen consumption rate (OCR) (A, D, G), extracellular acidification rate (ECAR) (B, E, H), and proton efflux rate (PER) (C, F, I) of HEK293 cells exposed to either vehicle (0.1% DMSO) or TDCIPP (0.061, 0.245, or 0.98 μM) for 24 h. Asterisk (*) denotes a significant difference ($p < 0.05$) relative to vehicle controls.

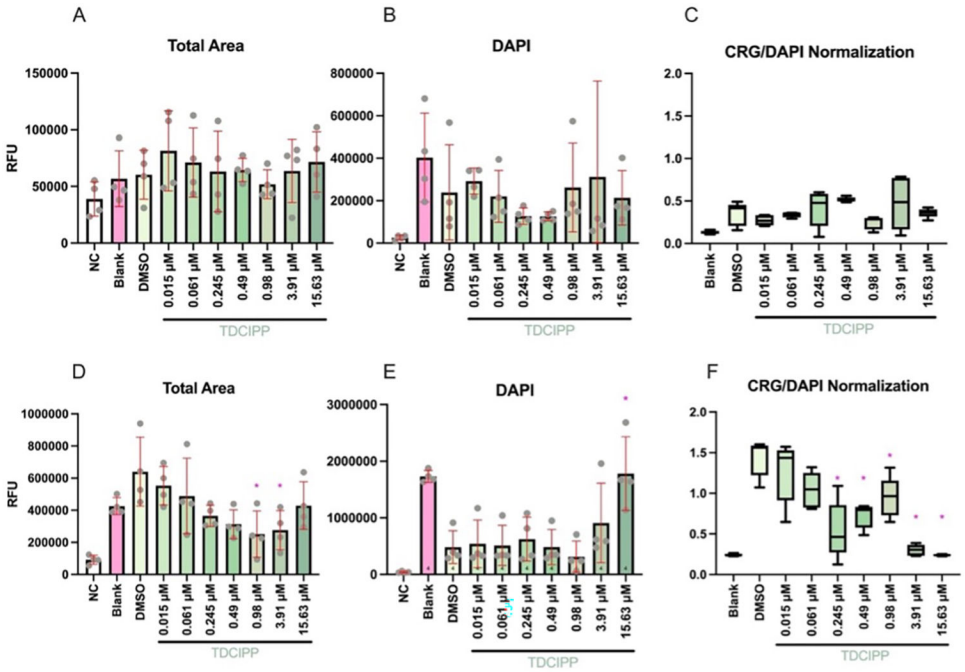

Fig. 5.

Mean (± standard deviation) CellROX Green fluorescence (A, D) and DAPI (B, E) of HEK293 cells exposed to either vehicle (0.1% DMSO) or 0.015–15.63 µM TDCIPP for 24 h (A-C) or 48 h (D-F). Blank = unexposed cells. Panels C and F show mean (± standard deviation) CellROX green fluorescence area divided by DAPI stained area of HEK293 cells. Asterisk (*) denotes a significant difference ($p < 0.05$) relative to vehicle controls.

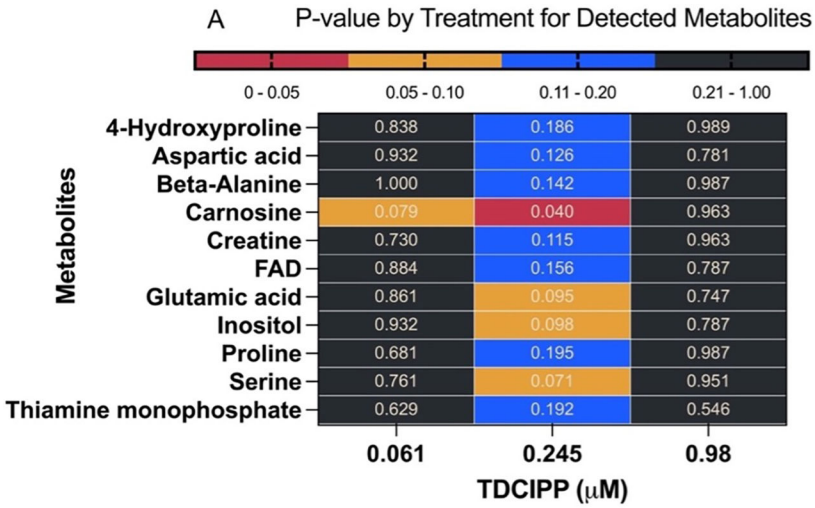

Fig. 6.

GLM-generated p-values for HEK293 cells exposed to either 0.061, 0.245, or 0.98 μM TDCIPP for 24 h. p-values are relative to vehicle-treated cells. Red color denotes a significant difference ($p < 0.05$) relative to vehicle controls.

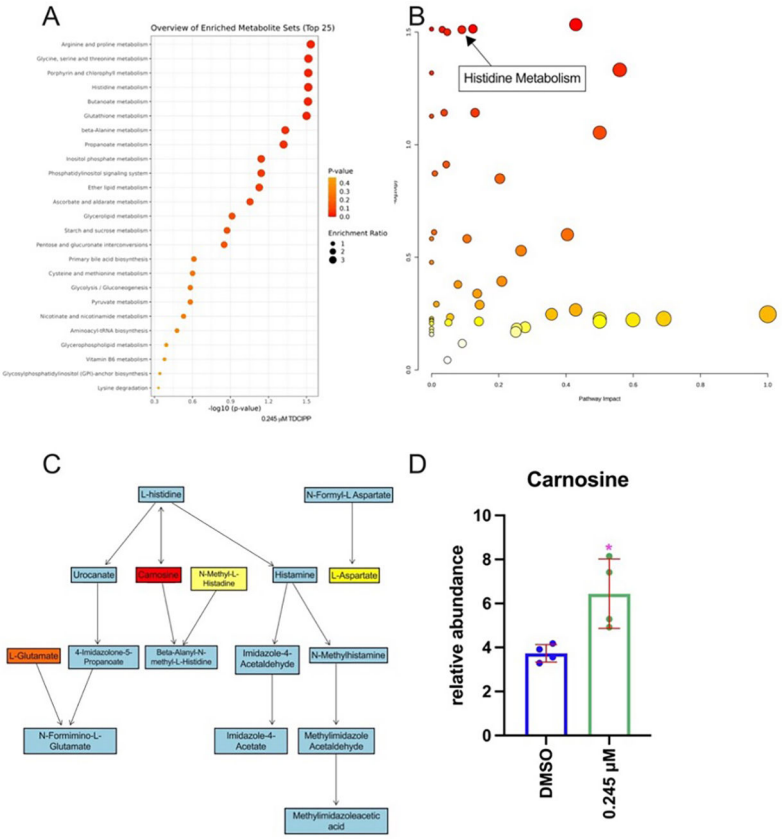

Fig. 7.

Significantly enriched metabolites (A) and pathway analysis (B) from MetaboAnalyst output. Histidine metabolism pathway from Panel B along with significantly affected metabolites (C). Mean (± standard deviation) carnosine relative abundance of HEK293 cells exposed to either vehicle (0.1% DMSO) or 0.245 µM TDCIPP for 24 h (D). Asterisk (*) denotes a significant difference ($p < 0.05$) relative to vehicle controls.

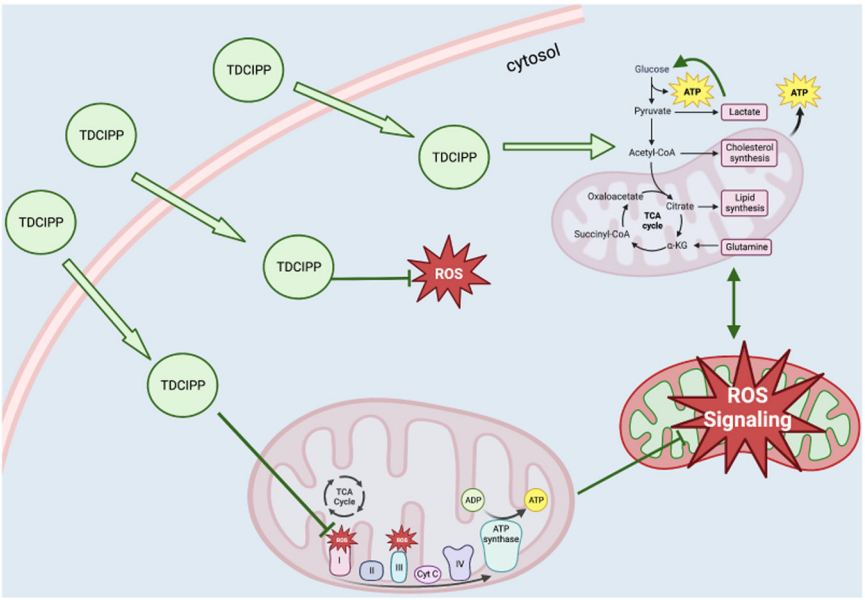

Fig. 8.

Proposed mechanisms of action for TDCIPP-induced disruption of metabolism within HEK293 cells.